

Quantum-computing within a bosonic context: Assessing finite basis effects on prototypical vibrational Hamiltonian spectra

Joachim Knapik,^{1,2} Bruno Senjean,² Benjamin Lasorne,^{2,*} and Yohann Scribano¹

¹*Laboratoire Univers et Particules de Montpellier, Université de Montpellier,
UMR-CNRS 5299, 34095 Montpellier Cedex, France*

²*ICGM, Univ Montpellier, CNRS, ENSCM, Montpellier, France*

Quantum computing has recently been emerging in theoretical chemistry as a realistic avenue meant to offer computational speedup to challenging eigenproblems in the context of strongly-correlated molecular systems or extended materials. Most studies so far have been devoted to the quantum treatment of electronic structure and only a few were directed to the quantum treatment of vibrational structure, which at the moment remains not devoid of unknowns. In particular, we address here a formal problem that arises when simulating a vibrational model under harmonic second quantization, whereby the disruption of the closure relation (resolution of the identity) – which occurs when truncating the infinite bosonic basis set – may have some serious effects as regards the correct evaluation of Hamiltonian matrix elements. This relates intimately to the normal ordering of products of ladder operators. In addition, we discuss the relevance of choosing an adequate primitive basis set within the present context with respect to its variational convergence properties. Such fundamental, yet consequential, aspects are illustrated numerically in the present work on a one-dimensional anharmonic Hamiltonian model corresponding to a double-well potential showing strong tunneling, of interest both for vibrational spectroscopy and chemical reactivity.

Keywords: quantum computing; Hamiltonian mapping; qubit encoding; ladder operators and normal order; bosonic modes; vibrational structure; tunneling in spectroscopy and chemistry.

I. INTRODUCTION

Quantum-computing (QC) techniques are nowadays believed to be promising computational alternatives compared to classical ones as regards the simulation of molecular properties, especially when the size and complexity of the problem makes it intractable on a classical computer [1]. In particular, electronic-structure calculations have been known to already benefit from significant algorithmic progress in QC [2–7]. In contrast, the simulations of molecular vibrational structure on a quantum computer are still in their infancy [8]. When doing QC on a qubit-based digital quantum computer, one often has to express the Hamiltonian within a second-quantized operator formulation via some kind of algebraic mapping that relies on the preliminary choice of a computational basis. While this is not mandatory, it is convenient, and this has been done in most of the cases addressed in the literature [9]. Such a formulation requires to know the action of the second-quantized operators with respect to the basis [10].

As regards the electronic-structure problem, the quantum-chemistry Hamiltonian has its universal and standard second-quantized definition with one- and two-body terms (Fock, Coulomb, and exchange integrals). It relies on the knowledge of a one-body basis set, the spin-orbitals (either primitive – atomic orbitals – or variationally optimal/canonical – molecular orbitals) and the subsequent definition of creation and annihilation operators governing the one or zero electronic occupation number

of each one-body spin-orbital involved within the many-body Slater determinants viewed as ordered lists of occupation numbers, referred to as occupation number vectors (ONVs). In this, going from first (Hilbert space) to second (Fock space) quantization implies that the existence of one electron – a physical-matter elemental particle that is a fermion of spin-1/2 – is fully identified to an occupation number one – a mode-excitation quasiparticle – of a spin-orbital that is to be viewed as a fermionic mode. Then, for each spin-orbital, the creation and annihilation operators of an electron in the mode are further mapped to the lowering and raising Pauli operators of a qubit-type system, *i.e.*, a two-level system isomorphic both to a spinless hard boson with zero and one states and to a spin-1/2 with up and down states. Hence, each spin-orbital in the ordered list is one-to-one mapped to a qubit in the string, *i.e.*, a site in the one-dimensional lattice of symbolic spins. Dealing with the many-fermion antisymmetric properties of Fermi-Dirac statistics with respect to permutations, according to the Pauli exclusion principle, is further ensured thanks to the Jordan-Wigner mapping [11], which involves a nonlocal antisymmetrization “pre-string” for the previous occupied spin-orbitals within the ordered list with respect to the spin-orbital of interest. This naturally turns the qubit string – first, a mere hard-bosonic chain of commuting spins-1/2 without further prescription – into an actual many-fermion ordered ONV that duly shares the antisymmetric properties of a Slater determinant represented as a normal-ordered product sequence of creation and annihilation operators acting on the fermionic vacuum state, according to Wick’s theorem [12].

In contrast, along the vibrational-structure side, such a one-to-one correspondence is less transparent. Differ-

* benjamin.lasorne@umontpellier.fr

ent vibrational Hamiltonian representations can be used depending on the problem being addressed [13, 14]. A natural way to define a vibrational Hamiltonian within a bosonic perspective (a potentially-coupled system of assumedly spinless and distinguishable vibrational modes, each able in principle to accommodate an infinite number of bosonic quanta, *i.e.*, mode-excitation quasiparticles: the vibrational bosons, sometimes referred to as “vibrons”) is found upon using a relevant model and its standard primitive basis such as the harmonic-oscillator one. Hence, the canonical commutation relation between the position and momentum operators yields a fully equivalent description in terms of standard bosonic ladder creation and annihilation operators. In addition, while this choice of basis is rarely the most compact one [10], it is numerically convenient, since it allows one to get analytic integrals for evaluating all monomial functions of the position or momentum operators within a finite polynomial Taylor expansion. Then, if one wants to use qubits here, the bosonic ladder operators should further be mapped to conventional strings of two-level raising and lowering Pauli operators, and various types of such algebraic or numeral bosonic-qubitization encodings (in particular, unary or binary) have been developed for this purpose [15, 16].

As already alluded to, the harmonic-oscillator basis has an infinite number of elements labelled by the number of vibrational bosons within the bosonic mode, but one always has to truncate it in practical computational approaches. Doing so, special care has to be taken as regards the ordering of products of the finite matrix representations of the bosonic ladder operators involved within the “polyladder” vibrational Hamiltonian matrix expansion. If not, even in the harmonic case, one thus simulates a fictitious system that is not only a finite variational approximation of the linear harmonic-oscillator model but – in fact – something else, with spurious eigenstates and eigenvalues, specifically named as the “truncated harmonic oscillator” model by Buchdahl in the 1960s, which actually implies a very modification of the canonical commutation rules [17]. Prototypical upper-bounded bosonic-like models such as the vibrational Morse oscillator, which really has a finite number of bound eigenstates, have been rationalized adequately over many decades along similar algebraic lines [18]. Yet, the numerical effect of such a predicament when truncating an anharmonic oscillator model that is not upper-bounded, for example a quartic double well, is not easily predictable and truly deserves some detailed analysis, which will be exposed in the present work.

At this stage, it remains evident that we may still encounter unexpected formal or numerical traps when applying QC to vibrational-structure problems without care, which justifies that some investigations of basic one-dimensional models must be carried out dutifully before going further. Along this line, various types of prototypical one-dimensional vibrational models have been explored recently within the QC framework [19]. Herein,

we focus on a double-well potential exhibiting fine splitting of its eigenvalues due to strong tunneling, of relevance for vibrational spectroscopy (*e.g.*, ammonia inversion [20–22]) or chemical reactivity (*e.g.*, hydrogen transfer in malonaldehyde [23]), with a nontrivial convergence behavior. The consequences of the basis truncation are investigated within the present work under two different scopes: the conventional variational convergence properties due to the nature and to the pruning of the finite basis, and how this translates within the QC framework in practice; the spurious effect of the disruption of the closure relation (resolution of the identity) and its relation to the so-called normal ordering when invoking product sequences of projected bosonic ladder operators.

The outline of our work is as follows. Some detailed conceptual background is given in the next section. We then provide essential information about the model and relevant computational details. The section before last is dedicated to results and discussion that highlight what can be taken as good practice for vibrational simulations when using QC, while at the same time assessing the question of the choice of the basis. We finish with concluding remarks and outlook. Extra information is given in Appendices for completion.

II. CONCEPTUAL BACKGROUND

The essential theoretical background required to address a vibrational system according to a bosonic framework and within the realm of QC is exposed in the present section. Additional details are provided in Appendix A. We shall show that a second-quantized form of the vibrational Hamiltonian in terms of bosonic ladder operators proves useful for further encoding its action with respect to a primitive basis set but implies some precautions when the basis is truncated within a computational context.

A. Encoding the vibrational problem on a quantum computer

The generic vibrational problem expressed in terms of L normal modes corresponds to the following multidimensional Hamiltonian in position representation (using mass-weighted rectilinear normal coordinates), assuming $\hbar = 1$,

$$\hat{H} = -\frac{1}{2} \sum_{i=1}^L \frac{\partial^2}{\partial x_i^2} + V(x_1, \dots, x_L) \quad . \quad (1)$$

We shall see further on that it can be mapped onto a quantum computer using different types of encodings. The most general second-quantized formulation maps each pair of position, \hat{x}_i , and momentum, \hat{p}_i , self-adjoint operators to an equivalent – non-self-adjoint, but mutu-

ally adjoint – pair of bosonic operators, \hat{b}_l and \hat{b}_l^\dagger , via

$$\begin{aligned}\hat{x}_l &= \frac{1}{\sqrt{2}}(\hat{b}_l + \hat{b}_l^\dagger) \quad , \\ \hat{p}_l &= \frac{1}{i\sqrt{2}}(\hat{b}_l - \hat{b}_l^\dagger) \quad ,\end{aligned}\quad (2)$$

such that the canonical commutation relation,

$$[\hat{x}_l, \hat{p}_k] = i\hat{1}\delta_{lk} \quad ,\quad (3)$$

translates into a standard bosonic commutation relation,

$$[\hat{b}_l, \hat{b}_k^\dagger] = \hat{1}\delta_{lk} \quad ,\quad (4)$$

where δ_{lk} denotes the Kronecker symbol. In the multidimensional direct-product harmonic-oscillator basis, these bosonic operators occur to be the second-quantized harmonic ladder, creation and annihilation, operators that act as

$$\begin{aligned}\hat{b}_l^\dagger |n_1 \dots n_l \dots n_L\rangle &= \sqrt{n_l + 1} |n_1 \dots n_l + 1 \dots n_L\rangle \quad , \\ \hat{b}_l |n_1 \dots n_l \dots n_L\rangle &= \sqrt{n_l} |n_1 \dots n_l - 1 \dots n_L\rangle \quad ,\end{aligned}\quad (5)$$

where the $\{|n_1 \dots n_l \dots n_L\rangle\}$ are the ONVs for L modes and $\sum_l n_l$ is the total number of harmonic bosons within any basic ONV. In contrast to the electronic-structure problem where the fermionic or hard-bosonic occupations can only be 0 or 1, the bosonic occupations n_l can be infinite in principle and – in practice – as large as the finite size of the basis, denoted by M_l for the l -th mode. Hence, a more-than-one bosonic occupation number cannot be encoded within a single qubit, as generally done in quantum chemistry using the Jordan–Wigner mapping for fermions [11]. Instead, the one-to-one use of L qudits of dimension M_l appears appealing, as well as the use of quomodes in continuous-variable QC. But, as qubits are more commonly used, L registers of several qubits are our focus herein to encode the more-than-one occupation numbers of the L bosonic modes. We shall further investigate the one-dimensional case where $L = 1$.

The simplest multi-qubit-based mapping for bosons [15] is called the direct or unary mapping [9, 10, 24] – also referred to as one-to-one [16], one-hot [24, 25], or single-excitation subspace [26] –, which consists in encoding the occupation of the l -th mode onto M_l qubits. Interestingly enough, such a unary-mapping approach can be traced back at least to 1997, during the pre-QC-era, with the seminal work of Thoss and Stock about the second-quantized theoretical treatment of vibronic phenomena [27, 28], which – together with the spin- S mapping of finite $(2S + 1)$ -state subspaces, earlier explored by Meyer and Miller [29] in 1979 – gave rise to what is now known as the MMST mapping within its own scientific context: namely, nonadiabatic semiclassical dynamics based on spin-boson diabatic Hamiltonian models. A detailed and illuminating review of algebraic dictionaries among various languages relating prototypical systems and

models of different types within a QC context has been proposed by Batista and Ortiz in 2004 [30].

Within the unary mapping, all qubit-states are set to 0 but the state of the n_l -th qubit, which is set to 1. This mapping is particularly noneconomic in terms of number of qubits, as one requires $\sum_l M_l$ qubits in total and a very sparse exploration of the symbolic Fock space (restricted here to a single quasiparticle). However, it is quite transparent as regards the transcription of the action of the multi-level bosonic ladder operators in terms of strings of two-level qubit operators. Indeed, within the unary mapping, the bosonic ladder operators are isomorphic to Kronecker direct products of raising and lowering qubit operators describing occupation transitions between first-neighbor pairs – also known as Ising interactions [15] – for any mode l ,

$$\hat{b}_l^\dagger = \sum_{r_l=0}^{M_l-2} \sqrt{r_l + 1} \hat{\sigma}_{r_l+1}^- \otimes \hat{\sigma}_{r_l}^+ \quad ,\quad (6)$$

which can be decomposed into only $O(M_l)$ local Pauli strings upon using the following algebraic equivalences,

$$\begin{aligned}\hat{\sigma}^- &\equiv \hat{a}^\dagger = |1\rangle \langle 0| \equiv \frac{1}{2}(X - iY) \quad , \\ \hat{\sigma}^+ &\equiv \hat{a} = |0\rangle \langle 1| \equiv \frac{1}{2}(X + iY) \quad ,\end{aligned}\quad (7)$$

where X and Y notations are the standard matrix representations of the $\hat{\sigma}_x$ and $\hat{\sigma}_y$ Pauli operators (also known as Pauli gates within a QC context) and are further detailed in Appendix B. Note that we are using here the spin-based convention for defining the raising and lowering Pauli operators, whereby the first qubit-state is $|0\rangle \equiv |\uparrow\rangle$ and the second qubit-state is $|1\rangle \equiv |\downarrow\rangle$ (hence, spin-lowering qubit-creates and spin-raising qubit-annihilates). The reverse convention is sometimes found in the literature. In addition, the nonlocal Jordan-like “pre-strings” of local identity operators acting on all qubits but the r_l and $r_l + 1$ ones within the full strings are transparent and have been made implicit for notational simplicity.

A more qubit-economic mapping is provided by the so-called compact mapping [9, 24], which is equivalent to a numeral binary encoding of each integer number n_l . Such an encoding has also been used in the context of electronic-structure theory to simulate a block of fixed-particle number in the second-quantized Hamiltonian, known as the configuration-interaction matrix [31–33], or to simulate non-interacting systems such as in quantum density-functional theory [34], Hückel theory [35], or the free-fermion problem [36]. There, only $K = \lceil \log_2(M_l) \rceil$ qubits, where $\lceil \cdot \rceil$ is the ceiling function, are required for the mode l but at the expense of having $O(M_l \log_2(M_l))$ nonlocal Pauli strings when decomposing the ladder operators,

$$\hat{b}_l^\dagger = \sum_{r_l=0}^{M_l-2} \sqrt{r_l + 1} |r_l + 1\rangle \langle r_l| \quad ,\quad (8)$$

with

$$|r_l\rangle = |c_{K-1}\rangle |c_{K-2}\rangle \dots |c_0\rangle \quad , \quad (9)$$

and the binary representation $r_l = c_{K-1}2^{K-1} + c_{K-2}2^{K-2} + \dots + c_02^0$ where $c_i \in \{0, 1\}$ for $0 \leq i \leq K-1$. In practice, this implies to choose some large enough value of K (number of qubits) such that $M_l = 2^K$ will be the actual size of the primitive basis for mode l . Combining Eqs. (7-9), each first-neighbor transition (jump) operator within the sum in Eq. (8) can be decomposed into $O(2^K) = O(M_l)$ nonlocal Pauli strings, thus leading to $O(M_l^2)$ Pauli strings for the ladder operator under compact encoding. However, there are $(2^K - (K + 1))2^K = M_l^2 - (\log_2(M_l) + 1)M_l$ redundant Pauli strings, thus leading to $O(M_l \log_2(M_l))$ Pauli strings only. Further details are provided in Appendix B.

Along the same line but somewhat alternatively, and as noticed by Ollitrault *et al.* [10], the direct/unary mapping has the nice advantage that it can be generalized symbolically to any type of computational basis with an unrestricted number of states: not only the harmonic-oscillator primitive basis, but potentially a variationally contracted one of VSCF (vibrational self-consistent field) type, aimed at being more compact. Indeed, we can always invoke strings of “abstract” second-quantized creation and annihilation qubit operators that do not have any evident first-quantized equivalent but that are defined only to make us navigate through a ladder way along the extent of the basis. Such a formulation has the advantage of making us able to rewrite the Hamiltonian in Eq. (1) under a many-body cluster-expansion form that is analog (except without the nonlocal Jordan-Wigner “pre-string” of Pauli Z) to the second-quantized electronic-structure problem [10],

$$\begin{aligned} \hat{H} = & \sum_{l=1}^L \sum_{k_l, h_l}^{M_l} \langle \varphi_{k_l} | \hat{T}_l + \hat{V}_l^{(1)} | \varphi_{h_l} \rangle \hat{a}_{k_l}^\dagger \hat{a}_{h_l} \\ & + \sum_{l < m}^L \sum_{k_l, h_l}^{M_l} \sum_{k_m, h_m}^{M_m} \langle \varphi_{k_l} \varphi_{k_m} | \hat{V}_{l,m}^{(2)} | \varphi_{h_l} \varphi_{h_m} \rangle \hat{a}_{k_l}^\dagger \hat{a}_{k_m}^\dagger \hat{a}_{h_l} \hat{a}_{h_m} \\ & + \dots \quad , \quad (10) \end{aligned}$$

where the first term is the one-body problem, which will be the main focus of the present work (where $L = 1$ because we shall be considering a one-dimensional model system). In the above equation, φ_{k_r} can be a one-body primitive harmonic-oscillator wavefunction or an optimized modal wavefunction obtained within a VSCF scheme. In this, the operators $\hat{a}_{k_l}^\dagger$ (\hat{a}_{k_l}) are the standard qubit mode-(de)excitation operators, also called hard-boson creation (annihilation) operators – which identify to the local spin-1/2 Pauli lowering (raising) operators on site k_l , *i.e.*, $\hat{a}_{k_l}^\dagger \equiv \hat{\sigma}_{k_l}^-$ and $\hat{a}_{k_l} \equiv \hat{\sigma}_{k_l}^+$ [see our previous remark about the spin-based convention whereby $|0\rangle \equiv |\uparrow\rangle$ and $|1\rangle \equiv |\downarrow\rangle$, which is conform to the standard definition of Pauli matrices]. They are thus fully related to the direct/unary mapping introduced previously for

mapping the bosonic ladder operators in Eqs. (5-6) but with respect to a potentially more general basis.

Now, and much as for the electronic-structure problem, we are facing the potential difficulty of evaluating numerically the integral factors in front of the qubit operators in Eq. (10), within the cluster-expansion hierarchy of one-body terms, two-body-terms, *etc.* There is a plethora of approaches for that, for example analytic quadrature techniques (according to specific primitive basis types). Numerical integral evaluations on grids are another option but they become rapidly prohibitive as the number of degrees of freedom increases, which is a striking example of what is known as the “curse of dimensionality” in vibrational-structure theory. Also, in contrast with electronic-structure theory – where the expression of the potential energy is known analytically from first principles (Coulombic interactions between point charges) – it must be stressed here that, in vibrational-structure theory, the global potential-energy function is only known first as a mere “numerical object” that is never given in advance and requires the evaluation of a large enough sample of its numerical values on a grid – obtained from numerous Born-Oppenheimer electronic-structure computations, or even beyond – to be made preliminarily and further fitted to a functional parametric ansatz (for example an anharmonic model). Such a requirement often represents some tedious work to be carried out first, which is beyond the scope of the present work.

Within the present study, we shall consider from the onset a one-dimensional potential-energy model involving polynomial powers of a single coordinate, up to degree four. Using a description in terms of the harmonic ladder operators \hat{b} and \hat{b}^\dagger [see Appendix A] will provide analytic expressions of the aforementioned integrals. At this stage it is perhaps important to make the following remark: while they are not totally disconnected from the overall mapping procedure, there are two very different types of second quantization here and they should not be confused together. The physical bosonic one with its harmonic ladder operators (\hat{b} and \hat{b}^\dagger) is there for two reasons: it is formally a natural algebraic way of expressing the vibrational Hamiltonian under a bosonic form when using a harmonic-oscillator primitive basis; it provides an easy avenue for numerically evaluating the matrix elements of the potential energy when expressed as a polynomial expansion with respect to the normal coordinate(s). Then, the formal hard-bosonic one, with its qubit operators (\hat{a} and \hat{a}^\dagger), is there for mapping (unarily or binarily) the multi-level problem onto a register of several two-level qubits within a QC context. In any case, both can be used together in practice for evaluating the integrals in Eq. (10) when using a harmonic-oscillator primitive basis. Going to qudits should eventually reconcile both approaches to some extent, which is left for further work because this raises additional and nontrivial questions (mapping a true bosonic infinite set to a more-than-two but finite set beyond qubit algebra).

B. Dealing with a finite basis

Below, we shall discuss the two types of errors that arise when truncating the primitive basis set within a QC context for some Hamiltonian models with *a priori* unknown eigensolutions.

First, there is a variational error that comes from using a finite basis to describe an infinitely large bosonic Hilbert/Fock space. The Hamiltonian operator is thus represented in practice by a matrix of finite size. This is unavoidable and manifests itself both in classical computing and QC. Such an error is tamed by the Rayleigh-Ritz variational principle: it is supposed to decrease monotonically when the size of the primitive basis increases, thus always yielding well-behaved convergence properties in principle but at some potentially significant computational cost. In this context, choosing a “good primitive basis set” for the problem at stake, *i.e.*, a parametrization that ensures efficient variational convergence properties as concerns the numerics, is an essential aspect; this will be addressed and illustrated with examples discussed in Section IV.

Second, there is a formal error that is not variational and merely due to the incomplete resolution of the identity when considering products of finite matrices involved in the expansion of the total Hamiltonian matrix. While we know how to avoid it formally when invoking representations based on normal-ordered products of harmonic ladder operators [see Appendix A], the numerical effect of this error is not trivial for a Hamiltonian that is beyond harmonic, and this remains of interest to be explored from a more general perspective. Indeed, one may be tempted to assume that such an error will have a negligible effect on the final eigenvalues. However, we shall show that it actually can break variationality quite dramatically and within an unpredictable manner. Hence, duly expressing the Hamiltonian using the normal order, which requires some additional pre-processing work, is a preliminary step that should never be avoided; this will also be explored in Section IV.

III. MODEL AND COMPUTATIONAL DETAILS

In order to assess the aforementioned issues against a practical situation of spectroscopic and chemical interest, we shall consider a prototypical one-mode model with a symmetrical double well describing strong tunneling. Its nondimensionalized Hamiltonian reads

$$\hat{H} = \hat{h}_0 - \frac{1}{2\ell} \hat{x}^3 + \frac{1}{8\ell^2} \hat{x}^4 \quad , \quad \hat{h}_0 = \frac{1}{2}(\hat{p}^2 + \hat{x}^2) \quad , \quad (11)$$

where \hat{h}_0 is the harmonic approximation of \hat{H} around the bottom of the left well (the origin: $x = 0$). The (dimensionless length) width of the barrier is $\delta = 2\ell$ and its (dimensionless energy) height is $\eta = \frac{\ell^2}{8}$. Here, we chose $\ell = 4$ [37]. Note that some energy rescaling will

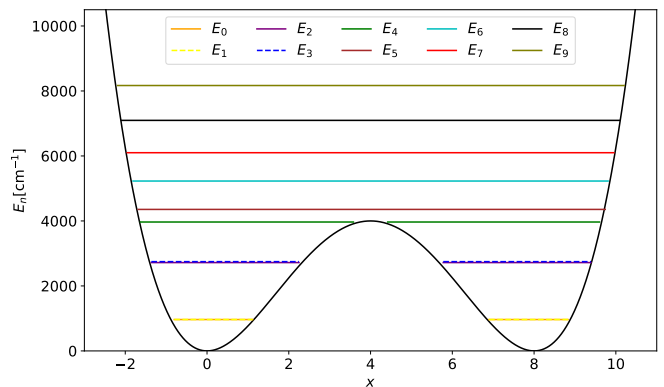


Figure 1: Double-well potential energy along the x coordinate, together with the first ten eigenvalues, E_n (given in cm^{-1}).

be considered hereafter for making things more concrete, with a harmonic frequency $\omega \equiv 0.0091127$ hartree $\equiv 2000$ cm^{-1} , which yields a barrier height of 4000 cm^{-1} .

For emulating a QC situation, the qubit-operator representation of the Hamiltonian was generated using the IBM Qiskit 0.45.1 software [38], with a binary encoding of the creation and annihilation operators [16] [further exemplified in Appendix B]. For a detailed analysis of the problems at stake, we also considered numerical full diagonalizations using LAPACK syevd libraries [39]. In this, the numerical-matrix representation of the Hamiltonian operator \hat{H} was assembled as a sum of products of matrix representations based on those of the \hat{b}^\dagger and \hat{b} operators, with their analytic expressions in the harmonic-oscillator primitive basis, and using different orderings (unordered and normal-ordered). Note that the values of the matrix elements of the powers of \hat{x} and \hat{p} can be compared to closed formulae, such as those derived for example by Chang [40].

The potential energy of our model, together with the first ten eigenvalues, are shown in Fig. 1, with an energy scaling factor $\hbar\omega \equiv 2000$ cm^{-1} . The first two tunneling eigenvalue pairs (0-1; 2-3) are below the transition barrier (4000 cm^{-1}). The following eigenvalue (4) is almost at the barrier. The next ones are above and start becoming dominated first by a quadratic-potential behaviour, then by a quartic-potential one where the consecutive energy gap keeps increasing gently.

IV. RESULTS AND DISCUSSION

In the present section, we provide and discuss illustrations of the numerical effects of the formal aspects that we have mentioned above.

A. Effect of the ordering

Considering the Hamiltonian given in Eq. (11), a direct expansion of all the monomials of the \hat{p} and \hat{x} operators yields an “unordered” representation with terms that contain various types of products of $\hat{b}^\dagger\hat{b}$ and $\hat{b}\hat{b}^\dagger$,

$$\begin{aligned} \hat{H}_{\text{unordered}} = & \frac{1}{2}(\hat{b}^\dagger\hat{b} + \hat{b}\hat{b}^\dagger) - \frac{1}{4\ell\sqrt{2}}(\hat{b}^3 + \hat{b}^2\hat{b}^\dagger + \hat{b}\hat{b}^\dagger\hat{b} + \hat{b}\hat{b}^{\dagger 2} \\ & + \hat{b}^\dagger\hat{b}^2 + \hat{b}^\dagger\hat{b}\hat{b}^\dagger + \hat{b}^\dagger\hat{b}^2\hat{b} + \hat{b}^\dagger\hat{b}^3) + \frac{1}{32\ell^2}(\hat{b}^4 + \hat{b}^3\hat{b}^\dagger + \hat{b}^2\hat{b}^\dagger\hat{b} \\ & + \hat{b}\hat{b}^\dagger\hat{b}^2 + \hat{b}^\dagger\hat{b}^3 + \hat{b}^2\hat{b}^\dagger\hat{b} + \hat{b}^\dagger\hat{b}^2 + \hat{b}\hat{b}^\dagger\hat{b}^2 + \hat{b}\hat{b}^\dagger\hat{b}^\dagger\hat{b} + \hat{b}^\dagger\hat{b}\hat{b}^\dagger\hat{b} \\ & + \hat{b}^\dagger\hat{b}^2\hat{b}^\dagger + \hat{b}^\dagger\hat{b}^2\hat{b} + \hat{b}^\dagger\hat{b}^3\hat{b} + \hat{b}^\dagger\hat{b}^2\hat{b}\hat{b}^\dagger + \hat{b}^\dagger\hat{b}\hat{b}^\dagger\hat{b} + \hat{b}\hat{b}^\dagger\hat{b}^2 + \hat{b}\hat{b}^\dagger\hat{b}^3 + \hat{b}^\dagger\hat{b}^4). \end{aligned} \quad (12)$$

Quite obviously, it involves all possible unordered products of \hat{b}^\dagger with \hat{b} and \hat{b} with \hat{b}^\dagger up to fourth order. In contrast, getting the expression of the “ordered” representation requires some preliminary reshuffling work based on the bosonic commutation relation. The result of Wick’s ordering procedure makes use, as much as possible, of the various instances of $\hat{n} = \hat{b}^\dagger\hat{b}$ in the expansion, such that

$$\begin{aligned} \hat{H}_{\text{ordered}} = & \frac{1}{2}(2\hat{n} + \hat{1}) - \frac{1}{4\ell\sqrt{2}}(\hat{b}^3 + 3\hat{n}\hat{b} + 3\hat{b} + 3\hat{b}^\dagger \\ & + 3\hat{b}^\dagger\hat{n} + \hat{b}^\dagger\hat{b}^3) + \frac{1}{32\ell^2}(\hat{b}^4 + 4\hat{n}\hat{b}^2 + 6\hat{b}^2 + 6\hat{b}^\dagger\hat{n}\hat{b} \\ & + 12\hat{n} + 3\hat{1} + 6\hat{b}^{\dagger 2} + 4\hat{b}^{\dagger 2}\hat{n} + \hat{b}^{\dagger 4}) . \end{aligned} \quad (13)$$

Both expressions are equivalent and exact, in principle, as long as we assume unlimited access to the infinite harmonic-oscillator basis. However, in practice (*i.e.*, using a truncated basis of finite size M associated to the projector $\hat{P}_M = \sum_{i=0}^{M-1} |i\rangle\langle i|$; see Appendix A), the variational approximation of $\hat{H}_{\text{unordered}}$, $\hat{P}_M\hat{H}_{\text{unordered}}\hat{P}_M$, will yield a nonvariational error when one goes as far as replacing within its expression each occurrence of \hat{b} and \hat{b}^\dagger by their own projected restrictions, $\hat{b}_M = \hat{P}_M\hat{b}\hat{P}_M$ and $\hat{b}_M^\dagger = \hat{P}_M\hat{b}^\dagger\hat{P}_M$. In contrast, doing such a “brutal” replacement within the variational approximation of \hat{H}_{ordered} , $\hat{P}_M\hat{H}_{\text{ordered}}\hat{P}_M$, remarkably preserves the variational principle because the potential error due to the incomplete resolution of the identity occurs to cancel out per construction, as proved in Appendix A. Of course, the same holds for their finite matrix representations. Let us emphasize here that even the harmonic part of the unordered projected operator, $\frac{1}{2}\hat{P}_M(\hat{b}^\dagger\hat{b} + \hat{b}\hat{b}^\dagger)\hat{P}_M$, which is approximated as $\frac{1}{2}(\hat{b}_M^\dagger\hat{b}_M + \hat{b}_M\hat{b}_M^\dagger)$ when considering an incomplete resolution of the identity, corresponds in fact to an artificial system with a spurious eigenvalue, which Buchdahl specifically named the “truncated harmonic oscillator model”, subject to an abnormal commutation relation [17]. In contrast, when doing the same to its ordered counterpart, we get $\hat{b}_M^\dagger\hat{b}_M + \frac{1}{2}\hat{P}_M = \hat{P}_M\hat{h}_0\hat{P}_M$, and we duly recover the correct variational approximation of $\hat{h}_0 = \hat{n} + \frac{1}{2}\hat{1}$ [see Appendix A]. It must be understood

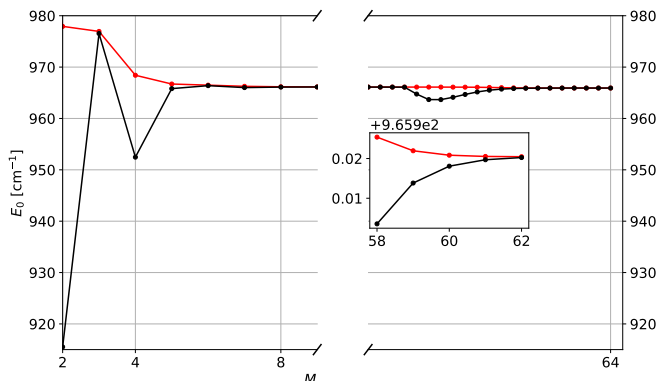


Figure 2: Convergence behavior of the lowest eigenvalue, E_0 (given in cm^{-1}) when increasing the total number of primitive basis functions, M , for both the ordered Hamiltonian (E_0^{ordered} ; in red) and the unordered one ($E_0^{\text{unordered}}$; in black).

that the present analysis is essential if one aims at building $\hat{P}_M\hat{H}\hat{P}_M$ as a sum of multiple products of \hat{b}_M^\dagger and \hat{b}_M , which are supposed to be available beforehand and ready in advance for further use according to some practical QC algorithmic conditions.

Let us consider what occurs when mapping \hat{b}_M^\dagger and \hat{b}_M to finite strings of Pauli operators. Again, to address the problem within a QC context, one first has to express each of the finite matrix representations of the bosonic ladder operators as a linear combination of Pauli strings (*i.e.*, a sum – with coefficients to be determined in advance thanks to the encoding procedure – of chains of Kronecker direct products of Pauli matrices). Using the aforementioned binary encoding [16] with three qubits yields 35 terms in the ordered case, for example. The unordered case also brings 35 terms, but totally different ones [see Appendix B], as expected from the previous discussion. This confirms that we actually are not representing the same system.

In what follows, we continue investigating the situation of an incomplete resolution of the identity (*i.e.*, \hat{b} and \hat{b}^\dagger are simply replaced beforehand by their restrictions, \hat{b}_M and \hat{b}_M^\dagger , within either $\hat{P}_M\hat{H}_{\text{unordered}}\hat{P}_M$ or $\hat{P}_M\hat{H}_{\text{ordered}}\hat{P}_M$). Then, the discrepancy between the ordered or unordered descriptions can be exemplified numerically upon inspecting the behavior of the lowest eigenvalue E_0 , obtained from exact diagonalization, and its convergence properties with respect to the size M of the harmonic-oscillator primitive basis. This is shown in Fig. 2.

As aforementioned, the behavior of E_0 with respect to the size of the primitive basis, M , is consistent with the variational principle in the ordered case (in red): it decreases smoothly and monotonically down to numerical convergence, which seems to occur visually for $M \approx 8$, but, in fact, truly occurs quite later on and only for $M \approx 60$ because we are dealing here with strong tunnel-

ing conditions (see later on for a more detailed analysis based both on eigenenergies and eigenstates). In contrast, it is evident that, in the unordered case (in black), the behavior of E_0 with respect to M is not variational at all. Indeed, several points are lower in energy than the converged solution (first, for $M < 8$ – and quite dramatically for $M = 2$ and $M = 4$ – and then again for $M \approx 50$). One could even be misled at believing that the problem were solved for $M \approx 46$ and be content, while a continued increase of the number of basis functions actually keeps making things worse upon creating a new unconverged deep after that. This is a clear manifestation of the issue related to a wrong ordering whereby the numerical system is polluted by spurious values of the matrix elements related to the abnormal commutation relations induced by an incomplete resolution of the identity.

Hence, even if recasting a nontrivial Hamiltonian according to the normal order may require some extra preliminary work, we stress that this is a task that should never be circumvented when one has to rely on a finite representation of the ladder operators beforehand. Our numerical illustration shows that the induced error is *a priori* not benign and should be taken seriously in general situations where its effect is difficult to predict, especially when convergence is entailed not to be rapid, such as in the present model that shows strong tunneling.

B. Effect of the primitive basis

Having sorted out the ordering issue, let us stick to a normal-ordered situation and now address the effect of the nature of the primitive basis. So far, we have been considering the primitive basis and its ladder operators as being attached to a harmonic Hamiltonian model with a given origin ($x = 0$) centered at the bottom of the left well of the anharmonic Hamiltonian model. It must be understood that this is a decision to be made in advance, and there are several other choices.

Determining a “good basis set” is essential in any quantum computational approach, and is crucial for QC, since the minimal number of basis functions used for converged simulations is ultimately related to the overall compactness of the quantum circuit, both in terms of width and depth: number of qubits and of operation gates (which has some significant impact on the primary sources of error due to extra noise because of additional opportunities of decoherence, for example). Hence, we checked here how some minimal change of definition (only shifting where the center of the basis is located) could potentially decrease the number of basis functions required for convergence. For this, we compared two different choices of origins for the same double-well model: at the bottom of the left well (as above) or, alternatively, at the central and symmetrical position of the top of the barrier between the left and right wells. The latter corresponds to a constant coordinate shift $x \mapsto x + 4\ell$ with respect to the original model.

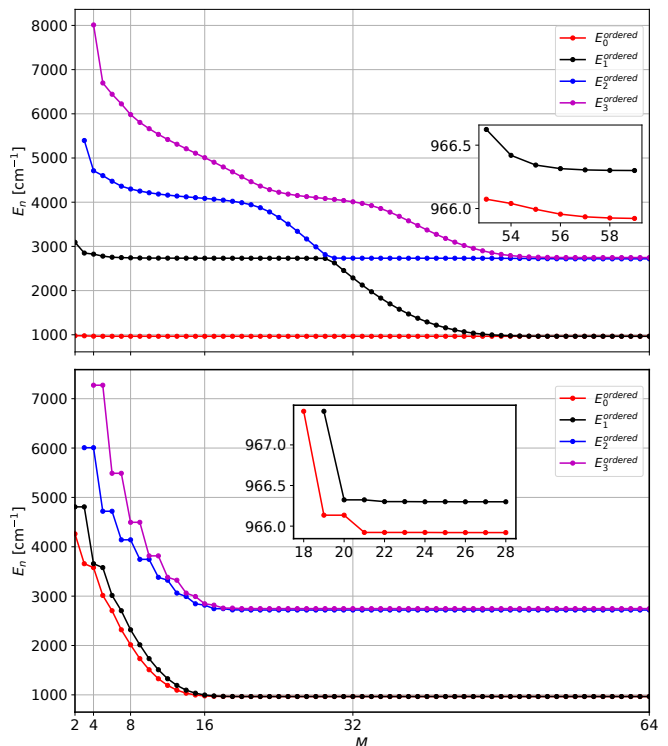


Figure 3: Behavior of the first four eigenvalues (given in cm^{-1}) when increasing the number of basis functions, M . The origin of the basis is located at the bottom of the left well, \hat{H}_{left} (top panel), or at the top of the barrier, \hat{H}_{center} (bottom panel).

Let us recall here that the choice of origin determines the very definition of \hat{x} , hence those of \hat{b} and \hat{b}^\dagger , which are intrinsically associated to a Gauss-Hermite basis centered at the current choice made for $x = 0$ (either the bottom of the left well or the top of the barrier). In practice, this thus leads to two different representations of the Hamiltonian of the same system, the one with the shifted potential energy now being

$$\hat{H}_{\text{center}} = \frac{1}{2}\hat{p}^2 + \frac{\ell^2}{8}\hat{1} - \frac{1}{4}\hat{x}^2 + \frac{1}{8\ell^2}\hat{x}^4 = \hat{h}_0 + \frac{\ell^2}{8}\hat{1} - \frac{3}{4}\hat{x}^2 + \frac{1}{8\ell^2}\hat{x}^4 \quad (14)$$

In the top panel of Fig. 3, which is associated to $\hat{H}_{\text{left}} = \hat{H}$ [see Eq. (11)], and as already mentioned, we observe that the lowest eigenvalue seems to be converging fast from visual inspection; however, the subtle effect of the tunneling splitting appears only for $M \approx 60$ basis functions, thus highlighting the strong anharmonicity of this model. In contrast, in the bottom panel of Fig. 3, we see that we converge both pairs of eigenvalues (0-1; 2-3) faster: the tunneling splitting is reached earlier, for $M \approx 22$ basis functions. A numerical example of the detailed convergence of the first five eigenvalues is given in Table I.

Then, analysing the convergence behavior of the weights of the lowest-energy eigenvectors (index n) with

Table I: First five eigenvalues in cm^{-1} of the Hamiltonian with the basis centered at the bottom of the left well (top table) and with the basis centered at the top of the central barrier (bottom panel). The index of the eigenvalues goes from 0 to 4 and the digits that differ from the reference values ($M = 128$) are highlighted in bold.

$E_{n,\text{left}}$		M					
n	56	58	60	62	64	128	
0	965. 9557	965.925 4	965.920 8	965.920 5	965.9204	965.9204	
1	966. 3429	966. 3046	966.299 9	966.299 6	966.2995	966.2995	
2	2718. 7273	2718. 4283	2718.377 1	2718.371 5	2718.371 3	2718.3712	
3	2747. 6837	2747. 3439	2747.287 1	2747.280 9	2747.2806	2747.2806	
4	3967. 8987	3967. 1728	3967.028 3	3967.009 2	3967.0078	3967.0078	

$E_{n,\text{center}}$		M					
n	24	26	28	30	32	128	
0	965.922 1	965.920 6	965.9204	965.9204	965.9204	965.9204	
1	966. 3002	966.299 6	966.2995	966.2995	966.2995	966.2995	
2	2718. 3813	2718.373 4	2718.371 3	2718.371 3	2718.3712	2718.3712	
3	2747.287 6	2747.281 0	2747.2806	2747.2806	2747.2806	2747.2806	
4	3967.023 1	3967.014 6	3967.008 0	3967.007 9	3967.0078	3967.0078	

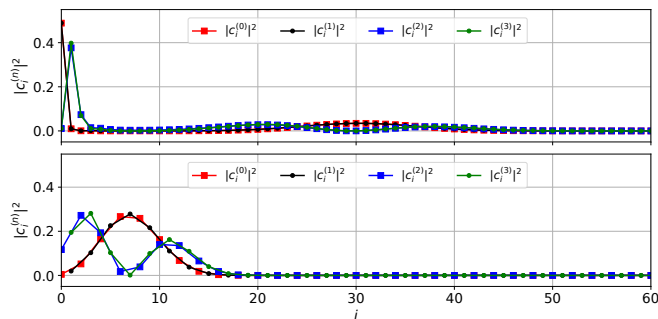


Figure 4: Behavior of the first four eigenstate weights at convergence with respect to the indices of the basis functions, i . The origin of the basis is at the bottom of left well, \hat{H}_{left} (top panel) or at the top of the barrier, \hat{H}_{center} (bottom panel).

respect to the basis functions (index i), $w_i^{(n)} = |c_i^{(n)}|^2 = |\langle i | \psi^{(n)} \rangle|^2$, for the two different origins of the bases is illuminating and is shown in Fig. 4. In the case where the basis is centered at the left well, most of the dominant contributions are recovered early on with a handful of basis functions. In particular, the ground ($n = 0$) and first-excited ($n = 1$) states of the first tunneling pair (about the normalized plus and minus combinations of the Gaussian functions of the left and right wells) are almost half-described by the single Gaussian function ($i = 0$) of the left well. Yet, because of strong tunneling, we have to wait for a while until we obtain the effect of the many detailed contributions of highly-excited basis functions, so as to reconstruct symmetrically the Gaussian contri-

bution in the right well from the excited states of the left well (typically peaking around $i \approx 30$ but with quite a large spread). As already mentioned, such a case is not trivial as regards convergence properties, which is why it was chosen as our focus here. However, such a behavior is not observed in the case where the basis is centered at the top of the barrier, for which we need to account for some early and large contributions, not beyond around $i \approx 20$). Hence, the latter case shows much better convergence properties. In addition, let us remark that this complies with symmetry considerations: even/odd eigenstates only expand over even/odd primitive states.

As a final word, it is interesting to analyse which type of Hamiltonian representation is bound to be more efficient numerically for a simulation based on a quantum algorithm. To this end, one can compare the one-norm of the qubit Hamiltonians, computed as the sum of the absolute values of the coefficients associated to the Pauli-string expansion of $\hat{H} = \sum_i \lambda_i \hat{P}_i$ as

$$\lambda = \sum_i |\lambda_i| \quad . \quad (15)$$

Indeed, the complexity of quantum algorithms typically scales with the one-norm, like the number of measurements in variational quantum algorithms [41] and in the simulation of the Hamiltonian using qubitization techniques [42, 43]. Changing the basis can have some significant impact on this quantity, as shown in Ref. [44] for the electronic-structure problem using localized orbitals. Similar studies are thus as much relevant for the vibrational-structure problem.

As readily seen in Fig. 5, the slope of the one-norms

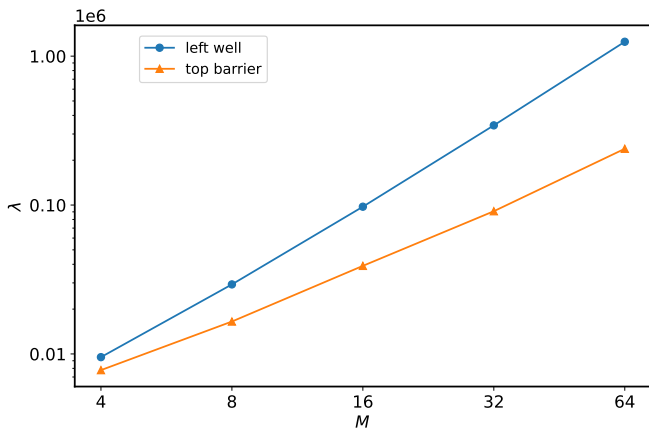


Figure 5: Behavior (log-log scale) of the one-norm λ of the Hamiltonians with the origin of the basis centered at the left-well bottom in blue or at the barrier top in orange, with respect to the number of basis functions M .

associated to the left-basis and center-basis are $\alpha = 1.76$ and $\alpha = 1.23$, respectively (in log-log scale). In addition, and according to Fig. 3, only 5 qubits (32 basis functions within the binary encoding) are required to converge the tunneling splitting when the basis is centered at the top of the barrier, while 6 qubits (64 basis functions) would be required when the basis is centered at the bottom of the left well. The one-norm for these two cases differs by one order of magnitude, in favor of the basis centered at the top of the barrier, which should therefore be preferred for a quantum simulation of the one-dimensional vibrational model presented in this work.

V. CONCLUSIONS AND OUTLOOK

After summarizing the essential theoretical background required for the application of qubit-based QC to vibrational-structure problems, we highlighted the fundamental issues that occur when the primitive basis is truncated in practice. Beyond the evident variational convergence properties with respect to the size of the finite basis, we also explored the less-known effect of various orderings of products of bosonic operators when defining the algebraic Hamiltonian representation to be mapped ultimately to qubits via unary or binary encodings. This was illustrated numerically on a one-dimensional Hamiltonian model corresponding to a nontrivial double-well potential showing strong tunneling and no upper bound, so as to drag attention onto the actual numerical effect of such a formal error, beyond the variational one, that may arise when simulating a vibrational problem on a quantum computer using a finite basis for a bosonic system with an infinite Hilbert space. We thus confirmed that using the so-called normal order is essential indeed and should never be circumvented, even if this requires extra preliminary work.

We also addressed the practical question of the optimal choice of a good basis set as regards the efficiency of variational convergence. In the case of a strongly anharmonic system, the first decision to be made is the location of the center of the primitive basis functions with respect to the origin of the potential energy function. This was illustrated here by a detailed analysis of convergence (eigenvalues and eigenvectors) comforted by an investigation of the one-norm, which relates to the efficiency of simulating vibrational-structure problems with QC algorithms.

We hope that the present work may benefit to researchers already doing vibrational structure with classical computing but aiming at exploring the capabilities offered by QC, as well as to researchers already doing QC for electronic structure but interested in generalizing their algorithms to vibrational structure.

DATA AVAILABILITY

No new data regarding actual systems were generated or analyzed in support of this study. The defining parameters of our models and the softwares and libraries that were used in our computations are all freely available and duly listed in the published article.

ACKNOWLEDGMENTS

We acknowledge the Institute for Quantum Technologies in Occitanie for its support through the PhD funding program AMI CMA QuantEDU-France (project ‘VibElQuant’). We warmly thank Saad Yalouz for regular discussions and relevant scientific input as regards the relevance of the present study.

Appendix A: Harmonic ladder operators and their properties

1. The harmonic oscillator prototype for a bosonic mode

Let us consider a generic, spinless, one-dimensional/one-particle quantum system. In what follows, we shall use nondimensionalized units (where, in particular, $\hbar = 1$). In the absence of any external field, such a system is determined by a time-independent and spin-free Hermitian Hamiltonian, \hat{H} , expressed as an analytic classical functional of its Hermitian position and momentum operators, \hat{x} and \hat{p} . The latter obey canonical commutation rules (responsible of the fundamental Heisenberg uncertainty principle),

$$[\hat{x}, \hat{p}] = i\hat{1} \quad , \quad (\text{A1})$$

where $\hat{1}$ is the identity operator of the system Hilbert space. Note that we implicitly assume vanishing bound-

ary conditions, such that being self-adjoint here boils down to being Hermitian. Then, we can define the following non-Hermitian operators,

$$\hat{b} = \frac{1}{\sqrt{2}}(\hat{x} + i\hat{p}) \quad , \quad \hat{b}^\dagger = \frac{1}{\sqrt{2}}(\hat{x} - i\hat{p}) \quad , \quad (\text{A2})$$

such that

$$\hat{x} = \frac{1}{\sqrt{2}}(\hat{b} + \hat{b}^\dagger) \quad , \quad \hat{p} = \frac{1}{i\sqrt{2}}(\hat{b} - \hat{b}^\dagger) \quad . \quad (\text{A3})$$

The latter are Hermitian; they obviously correspond to complex-conjugate phase-space variables and are often invoked within the context of coherent states (eigenstates of \hat{b}). The corresponding bosonic commutation rule follows from Eq. (A1) and reads

$$[\hat{b}, \hat{b}^\dagger] = \hat{1} \quad . \quad (\text{A4})$$

Now, it occurs that \hat{b} and \hat{b}^\dagger act as the ladder operators of the quantum harmonic-oscillator model with respect to its Fock space. This provides a natural primitive basis set in which the actions of the various ladder operators and their products can be made explicit. The nondimensionalized harmonic Hamiltonian model reads

$$\hat{h}_0 = \frac{1}{2}(\hat{p}^2 + \hat{x}^2) \quad , \quad (\text{A5})$$

with natural harmonic units (energy measured in terms of $\hbar\omega$, length in terms of $\sqrt{\frac{\hbar}{m\omega}}$, and momentum in terms of $\sqrt{\hbar m\omega}$; this implies to take $\hbar = 1$, $m = 1$, and $\omega = 1$ in practice). The eigenfunctions of the quantum harmonic-oscillator model in position representation are the Gauss-Hermite functions,

$$\langle x|n\rangle = \phi_n(x) = \frac{1}{\sqrt{\pi^{1/2}2^n n!}} e^{-\frac{x^2}{2}} \mathcal{H}_n(x) \quad , \quad (\text{A6})$$

where \mathcal{H}_n is the physicists' Hermite polynomial of degree n , for any $n \in \{0, 1, 2, \dots, \infty\}$.

As regards the harmonic basis set, $\{|n\rangle\}_{n=0}^\infty$, we have the following properties with respect to \hat{b} and \hat{b}^\dagger , for any nonnegative integer n ,

$$\hat{b}^\dagger|n\rangle = \sqrt{n+1}|n+1\rangle \quad , \quad (\text{A7})$$

$$\hat{b}|n\rangle = \sqrt{n}|n-1\rangle \quad , \quad (\text{A8})$$

augmented for consistency by the terminating ‘‘quantum vacuum’’ condition,

$$\hat{b}|0\rangle \equiv 0 \quad . \quad (\text{A9})$$

Further, we have the number operator, $\hat{n} = \hat{b}^\dagger\hat{b}$, which brings

$$\hat{n}|n\rangle = n|n\rangle \quad . \quad (\text{A10})$$

This allows us to establish a one-to-one correspondence between the Hilbert space of the vibrational system and the Fock space of the bosonic mode upon considering the index of the harmonic eigenvector, n , as the number of bosons in the harmonic mode.

It must be stressed here that the bosonic commutation relations still hold whether the actual Hamiltonian \hat{H} is the harmonic one, \hat{h}_0 , or something more complicated whereby $\{|n\rangle\}_{n=0}^\infty$ is no longer the eigenbasis but merely some primitive basis. Hence, for an anharmonic Hamiltonian, the harmonic ladder operators are no longer the bosonic ladder operators of the eigenbasis but only the bosonic ladder operators attached to the primitive harmonic-oscillator (Gauss-Hermite) basis. Yet, knowing the actions of \hat{b} and \hat{b}^\dagger with respect to the primitive basis allows us to determine conveniently the actions of \hat{x} and \hat{p} , and of any of their powers involved in a Hamiltonian that can be written as an analytic functional of those. In particular, in the present work, we have explored a situation where the kinetic-energy operator remains $\frac{1}{2}\hat{p}^2$ (rectilinear coordinate) but where the potential-energy operator is a confining lower-bounded quartic polynomial of \hat{x} .

Now, expressing \hat{p}^2 and \hat{x}^2 directly in terms of the harmonic ladder operators [direct expansion from Eq. (A3)] yields

$$\hat{h}_0 = \frac{1}{2}(\hat{b}^\dagger\hat{b} + \hat{b}\hat{b}^\dagger) \quad . \quad (\text{A11})$$

While such an expression seems perfectly valid at first sight, it brings potential sources of error when implementing it in practice for a truncated basis set (this will be discussed in the next subsection). From the commutation rule set in Eq. (A4), we can devise two alternative, and *a priori* equivalent, expressions of \hat{h}_0 ,

$$\hat{h}_0 = \frac{1}{2}(2\hat{b}^\dagger\hat{b} + \hat{1}) = \frac{1}{2}(2\hat{b}\hat{b}^\dagger - \hat{1}) \quad . \quad (\text{A12})$$

Within the second-quantized context of Wick's theorem [12], the first expression is known as ‘‘normal ordered’’, while the second as ‘‘antinormal ordered’’. Again, they are both equally valid in principle, but the ‘‘normal ordered’’ one is often preferred because it treats the quantum vacuum state in a more consistent manner. In any case, using the definition of the bosonic counting (quantum number) operator, it brings the well-known second-quantized form of the nondimensionalized harmonic Hamiltonian model,

$$\hat{h}_0 = \frac{1}{2}(2\hat{b}^\dagger\hat{b} + \hat{1}) = \hat{n} + \frac{1}{2}\hat{1} \quad . \quad (\text{A13})$$

Obviously, \hat{h}_0 and \hat{n} commute and share the same set of eigenvectors, which satisfy

$$\hat{h}_0|n\rangle = \left(n + \frac{1}{2}\right)|n\rangle \quad . \quad (\text{A14})$$

2. Truncation issues for finite basis sets

The harmonic-oscillator basis, defined above as $\{|n\rangle\}_{n=0}^{\infty}$, and attached to \hat{b} and \hat{b}^\dagger as its ladder operators, is discrete but infinite. However, under practical instances, it will have to be truncated so as to provide finite matrix representations of relevant operators. As shown below, there is a fundamental issue that concerns the truncated representation of a product of two operators with a finite matrix and whether or not it can be identified to the product of two such finite matrices.

We shall refer to $M > 0$ as the finite number of basis functions under computational circumstances. Restricted operators can be expressed upon using the idempotent projector: $\hat{P}_M = \sum_{i=0}^{M-1} |i\rangle\langle i|$ where $\hat{P}_M^2 = \hat{P}_M$. The truncated matrix representations of the operators will have an $(M \times M)$ -dimension. Formally, the corresponding projected ladder operators read

$$\hat{b}_M = \hat{P}_M \hat{b} \hat{P}_M \quad , \quad \hat{b}_M^\dagger = \hat{P}_M \hat{b}^\dagger \hat{P}_M \quad . \quad (\text{A15})$$

The problem at stake here is that

$$[\hat{b}_M, \hat{b}_M^\dagger] \neq \hat{P}_M \quad . \quad (\text{A16})$$

Note that \hat{P}_M is to be viewed as the projected representation of the identity operator within the finite subspace: $\hat{P}_M = \hat{P}_M \hat{1} \hat{P}_M \equiv \hat{1}_M$. Hence, we can no longer use the standard bosonic commutation relation to switch safely from some choice of ordering to another within the truncated subspace.

The proof is simple and follows. First, upon expanding the projectors involved within $\hat{b}_M^\dagger \hat{b}_M$, we get

$$\begin{aligned} \hat{P}_M \hat{b}^\dagger \hat{P}_M \hat{b} \hat{P}_M &= \sum_{i=0}^{M-1} \sum_{j=0}^{M-1} \sum_{k=0}^{M-1} |i\rangle\langle i| \hat{b}^\dagger |j\rangle\langle j| \hat{b} |k\rangle\langle k| \\ &= \sum_{i=0}^{M-1} \sum_{j=0}^{M-1} \sum_{k=0}^{M-1} |i\rangle\langle i| j+1 \rangle \langle j+1| \langle j+1| k \rangle \langle k| \\ &= \hat{P}_M |0\rangle\langle 0| \hat{P}_M + \hat{P}_M |M\rangle\langle M| M \langle M| \hat{P}_M \\ &\quad + \sum_{i=0}^{M-1} \sum_{l=1}^{M-1} \sum_{k=0}^{M-1} |i\rangle\langle i| l \rangle \langle l| \langle l| k \rangle \langle k| \\ &= \hat{P}_M \hat{n} \hat{P}_M \\ &= \hat{P}_M \hat{b}^\dagger \hat{b} \hat{P}_M \quad , \end{aligned} \quad (\text{A17})$$

where we used $l = j + 1$, the fact that incorporating $|0\rangle\langle 0|$ into the sum is merely adding up zero, and the property that $\hat{P}_M |M\rangle \equiv 0$ (orthogonality of the subspace with respect to its complement). Second, for $\hat{b}_M \hat{b}_M^\dagger$, we

have

$$\begin{aligned} \hat{P}_M \hat{b} \hat{P}_M \hat{b}^\dagger \hat{P}_M &= \sum_{i=0}^{M-1} \sum_{j=0}^{M-1} \sum_{k=0}^{M-1} |i\rangle\langle i| \hat{b} |j\rangle\langle j| \hat{b}^\dagger |k\rangle\langle k| \\ &= 0 \hat{P}_M + \sum_{i=0}^{M-1} \sum_{j=1}^{M-1} \sum_{k=0}^{M-1} |i\rangle\langle i| j-1 \rangle \langle j-1| \langle j-1| k \rangle \langle k| \\ &= \sum_{i=0}^{M-1} \sum_{l=0}^{M-2} \sum_{k=0}^{M-1} |i\rangle\langle i| l \rangle \langle l+1| \langle l+1| k \rangle \langle k| \\ &= \sum_{i=0}^{M-1} \sum_{l=0}^{M-1} \sum_{k=0}^{M-1} |i\rangle\langle i| l \rangle \langle l+1| \langle l+1| k \rangle \langle k| \\ &\quad - \sum_{i=0}^{M-1} \sum_{k=0}^{M-1} |i\rangle\langle i| M-1 \rangle \langle M-1| M \langle M-1| k \rangle \langle k| \\ &= \hat{P}_M (\hat{n} + \hat{1}) \hat{P}_M - \hat{P}_M |M-1\rangle\langle M-1| M \langle M-1| \hat{P}_M \\ &= \hat{P}_M \hat{b} \hat{b}^\dagger \hat{P}_M - |M-1\rangle\langle M-1| M \langle M-1| \quad , \end{aligned} \quad (\text{A18})$$

where we used the vacuum condition and $l = j - 1$. The last term is the culprit: it is now nonzero since it belongs to the truncated subspace. It follows that

$$[\hat{b}_M, \hat{b}_M^\dagger] = \hat{P}_M - |M-1\rangle\langle M-1| M \langle M-1| \neq \hat{P}_M \quad . \quad (\text{A19})$$

For illustrating purposes, let us consider a matrix representation, with $\mathbf{b}_M^\dagger \mathbf{b}_M$ and $\mathbf{b}_M \mathbf{b}_M^\dagger$ for $M = 4$, the elements of which being analytic integrals that are known explicitly. Their normal-ordered and antinormal-ordered products are, respectively,

$$\mathbf{b}_4^\dagger \mathbf{b}_4 = \begin{bmatrix} 0 & 0 & 0 & 0 \\ 0 & 1 & 0 & 0 \\ 0 & 0 & 2 & 0 \\ 0 & 0 & 0 & 3 \end{bmatrix} = \mathbf{n}_4 \quad (\text{A20})$$

and

$$\mathbf{b}_4 \mathbf{b}_4^\dagger = \begin{bmatrix} 1 & 0 & 0 & 0 \\ 0 & 2 & 0 & 0 \\ 0 & 0 & 3 & 0 \\ 0 & 0 & 0 & 0 \end{bmatrix} = \mathbf{n}_4 + \mathbf{1}_4 - \begin{bmatrix} 0 & 0 & 0 & 0 \\ 0 & 0 & 0 & 0 \\ 0 & 0 & 0 & 0 \\ 0 & 0 & 0 & 4 \end{bmatrix} . \quad (\text{A21})$$

This also modifies consistently the canonical commutation relation between the projected position and momentum operators,

$$[\hat{x}_M, \hat{p}_M] = i(\hat{P}_M - |M-1\rangle\langle M-1| M \langle M-1|) \neq i \hat{P}_M \quad , \quad (\text{A22})$$

where

$$\hat{x}_M = \hat{P}_M \hat{x} \hat{P}_M \quad , \quad \hat{p}_M = \hat{P}_M \hat{p} \hat{P}_M \quad . \quad (\text{A23})$$

Such a predicament, which was revisited in 2003 within a QC context by Somma *et al.* [15] – and further explored algebraically by Batista and Ortiz in 2004 [30] – was pointed out by Buchdahl as early as 1967 within the general framework of the so-called “truncated harmonic

oscillator model” [17]. There, it was noticed that the truncated harmonic Hamiltonian defined as

$$\hat{h}_{0M} = \frac{1}{2}(\hat{p}_M^2 + \hat{x}_M^2) \quad , \quad (\text{A24})$$

together with its abnormal canonical commutation relation (see above), could be reconsidered formally as sharing the algebraic properties of a finite angular-momentum Hamiltonian. Such a correspondence resonates directly with the seminal works of Jordan [45] in 1935 and Schwinger [46] in 1952 about the formal mapping to be made between the $\mathfrak{su}(2)$ Lie algebra of angular momenta ($|j, m\rangle$ states) and the bosonic Weyl algebra of two uncoupled truncated harmonic modes ($|n_1, n_2\rangle$ states), which was explored somewhat complementarily in 1940 by Holstein and Primakoff [47], upon realizing that fixing j to some nonnegative integer or half-integer value according to the irreducible representations of the $SU(2)$ Lie group, and letting m vary among $2j + 1$ values such that $-j \leq -j + 1 \leq \dots \leq m \leq \dots \leq j - 1 \leq j$, reduces the system to a single truncated harmonic mode, thanks to the conservation – as a constant of motion – of the so-called ‘polyad’: $n_1^2 + n_2^2$ [28]. The literature on this subject is vast [27–30, 48], and an exhaustive survey is beyond the scope of the present work; let us, however, mention some recent work [24] in 2020, reconsidering within a QC context the MMST-like mapping [27–29] between a finite $(2j + 1)$ -state bosonic-like Hamiltonian and a spin- j angular-momentum Hamiltonian, together with their relations via the $\mathfrak{su}(2)$ Lie algebra, the j -representations of the $SU(2)$ Lie group, and the generators of the $SU(2j + 1)$ Lie group [30].

Again, and as regards the present work, it should be understood that – on practical terms – the problem is somewhat simpler and can be viewed essentially as an incomplete resolution of the identity (also known as the closure relation) for an infinite Hilbert space when inserting a finite projector within a product of two operators. We can summarize the second-quantized description of a truncated bosonic mode with a finite set of ladder operators according to the scheme presented in Fig. 6.

Whether the basis is truncated or not, \hat{b} is lower-bounded by the $|0\rangle$ state (the “physical vacuum”). The basis truncation also implies that applying the creation operator to the last state of the truncated basis leads to a state that is not included in the truncated space. Thus, this creates an upper bound to the number of bosons that can be created in the mode, and a sort of extra “numerical vacuum” from above. As shown above, a solution is found when invoking the “normal ordered” product, $\hat{b}_M^\dagger \hat{b}_M = \hat{P}_M \hat{b}^\dagger \hat{P}_M \hat{b} \hat{P}_M = \hat{P}_M \hat{b}^\dagger \hat{b} \hat{P}_M = \hat{P}_M \hat{n} \hat{P}_M$, while using any type of “unordered” product causes troubles. Such a situation is general and applies to monomials of higher degree. Using Wick’s normal order is thus a practical recipe that allows us to avoid ill-defined situations.

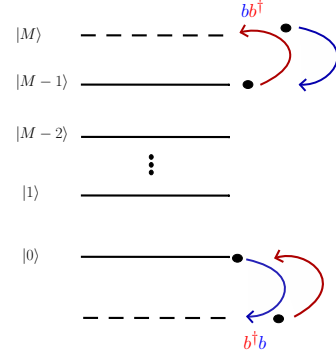


Figure 6: Schematic description of the action of bosonic ladder operator products with respect to a truncated harmonic-oscillator basis.

Appendix B: Binary qubit-mapping of the bosonic Hamiltonian

The so-called compact mapping [16] associates the bosonic Fock states to qubit strings according to a numerical binary mapping. For a total number of qubits denoted K , and starting counting from the right, we have the following mapping,

$$\begin{aligned} |0\rangle &= |0_1, 0_2, \dots, 0_{K-1}, 0_K\rangle \quad , \\ |1\rangle &= |0_1, 0_2, \dots, 0_{K-1}, 1_K\rangle \quad , \\ |2\rangle &= |0_1, 0_2, \dots, 1_{K-1}, 0_K\rangle \quad , \\ |3\rangle &= |0_1, 0_2, \dots, 1_{K-1}, 1_K\rangle \quad , \\ &\vdots \\ |2^K - 1\rangle &= |1_1, 1_2, \dots, 1_{K-1}, 1_K\rangle \quad . \end{aligned} \quad (\text{B1})$$

In order to show why the ladder operator in Eqs. (8-9) is decomposed into a linear combination of $O(M_l \log_2(M_l))$ (potentially nonlocal) Pauli strings only, we have to count the unique types of bit-flip patterns in all the $(M_l - 1)$ first-neighbor transition (jump) operators, $|r_l + 1\rangle \langle r_l|$. We shall simply call them projectors in what follows. The key insight is that the number of projectors having a unique type of bit-flip pattern corresponds to the number of possible lengths of trailing 1s within a K -bit binary integer, which is exactly $K = \log_2(M_l)$, *i.e.*, following a logarithmic scaling with the number of basis functions. Indeed, adding 1 to a binary number primarily affects the rightmost 0-bit by flipping it to 1. However, if there is a sequence of trailing 1s, all those 1s flip to 0, and the first 0-bit that is encountered flips to 1. Since a K -bit number can have at most K different lengths of trailing 1s (ranging from 0 to $K - 1$ trailing 1s), the number of unique transition patterns is at most $K = \log_2(M_l)$. Thus, there are exactly $\log_2(M_l)$ different patterns of bit flips, each of them giving $2^K = M_l$ different Pauli strings, finally totalling into $M_l \log_2(M_l)$ unique Pauli strings. Let us give an example for three qubits. The numbers of projectors $|r_l + 1\rangle \langle r_l|$ are $2^3 - 1 = 7$ and

are given as

$$\begin{aligned} & \{ |001\rangle \langle 000|, |010\rangle \langle 001|, |011\rangle \langle 010|, |100\rangle \langle 011|, \\ & |101\rangle \langle 100|, |110\rangle \langle 101|, |111\rangle \langle 110| \} . \end{aligned} \quad (\text{B2})$$

Only three unique patterns of bit flips arise from these seven projectors, grouped as follows. First, the first qubit passes from state 0 to 1, thus leading to

$$\begin{aligned} & \{|001\rangle \langle 000|, |011\rangle \langle 010|, |101\rangle \langle 100|, |111\rangle \langle 110|\} \\ & \rightarrow (I \pm Z) \otimes (I \pm Z) \otimes (X - iY) , \end{aligned} \quad (\text{B3})$$

where we used Eq. (7) as well as

$$\begin{aligned} |0\rangle \langle 0| & \equiv I^+ = \frac{1}{2}(I + Z) , \\ |1\rangle \langle 1| & \equiv I^- = \frac{1}{2}(I - Z) . \end{aligned} \quad (\text{B4})$$

Hence, those four different projectors share the same $2^3 = 8$ Pauli strings, up to relative phase factors within their linear combinations. Second, the state of the first qubit passes from 1 to 0, and the second from 0 to 1, thus leading to

$$\begin{aligned} & \{|010\rangle \langle 001|, |110\rangle \langle 101|\} \\ & \rightarrow (I \pm Z) \otimes (X - iY) \otimes (X + iY) , \end{aligned} \quad (\text{B5})$$

i.e., two projectors share the same eight Pauli strings. Finally, the last projector corresponds to a change in the state of the three qubits,

$$|100\rangle \langle 011| = (X - iY) \otimes (X + iY) \otimes (X + iY), \quad (\text{B6})$$

and thus does not share any of its eight possible Pauli strings with another projector. It is now clear from Eqs. (B3), (B5), and (B6) that the creation ladder operator can be written as a linear combination of at most $M_l \log_2(M_l)$ Pauli strings.

Interestingly, the decomposition of the restricted (finite-basis projection) bosonic creation operator \hat{b}_{k+1}^\dagger into a linear combination of Pauli string can also be obtained by a recursive relation [16],

$$\begin{aligned} \hat{b}_{k+1}^\dagger & = \sum_{i=1}^{2^k-1} \sqrt{i} I_1^+ \otimes \hat{c}_i^{(2,k+1)} + \\ & \sqrt{2^k} \hat{\sigma}_1^- \otimes \hat{\sigma}_2^+ \dots \otimes \hat{\sigma}_{k+1}^+ + \sum_{i=2^{k+1}}^{2^{k+1}-1} \sqrt{i} I_1^- \otimes \hat{c}_i^{(2,k+1)} . \end{aligned} \quad (\text{B7})$$

Here, for notational simplicity, we identify Pauli operators to Pauli matrices since there is no ambiguity. The symbolic notation $\hat{c}_i^{(2,k+1)}$ is meant to collect together all operators acting from qubit 2 to qubit $k+1 \leq K$. In practice, for $k=0$, we have $\hat{b}_1^\dagger = \hat{\sigma}_1^-$, which induces, for $k=1$,

$$\hat{b}_2^\dagger = I_1^+ \otimes \hat{\sigma}_2^- + \sqrt{2} \hat{\sigma}_1^- \otimes \hat{\sigma}_2^+ + \sqrt{3} I_1^- \otimes \hat{\sigma}_2^- , \quad (\text{B8})$$

and, for $k=2$,

$$\begin{aligned} \hat{b}_3^\dagger & = I_1^+ \otimes I_2^+ \otimes \hat{\sigma}_3^- + \sqrt{2} I_1^+ \otimes \hat{\sigma}_2^- \otimes \hat{\sigma}_3^+ + \sqrt{3} I_1^+ \otimes I_2^- \otimes \hat{\sigma}_3^- \\ & + \sqrt{4} \hat{\sigma}_1^- \otimes \hat{\sigma}_2^- \otimes \hat{\sigma}_3^+ + \sqrt{5} I_1^- \otimes I_2^+ \otimes \hat{\sigma}_3^- \\ & + \sqrt{6} I_1^- \otimes \hat{\sigma}_2^- \otimes \hat{\sigma}_3^+ + \sqrt{7} I_1^- \otimes I_2^- \otimes \hat{\sigma}_3^- . \end{aligned} \quad (\text{B9})$$

The $\hat{c}_i^{(2,k+1)}$ operators in \hat{b}_3^\dagger are thus $\hat{c}_1^{(2,3)} = I_2^+ \otimes \hat{\sigma}_3^-$, $\hat{c}_2^{(2,3)} = \hat{\sigma}_2^- \otimes \hat{\sigma}_3^+$, $\hat{c}_3^{(2,3)} = I_2^- \otimes \hat{\sigma}_3^-$, and so on for larger values of k [16].

Then, the square-root factors are regrouped to produce the actual coefficients of the Pauli strings, λ_i , which are implied in the expansion $\hat{H} = \sum_i \lambda_i \hat{P}_i$, where $\hat{P}_i = \bigotimes_j \hat{\sigma}_j$ for $i \in \{0, \dots, M-1\}$, and such that $\hat{\sigma}^j \in \{I, X, Y, Z\}$. As a matter of example, the Hamiltonian models given in Eqs. (12-13) thus correspond to the two following Hamiltonian matrices,

$$\begin{aligned} H_{\text{unordered}} & = 7355.49 III - 1070.32 IZZ - 3226.57 ZII \\ & - 1046.88 ZIZ - 1054.69 ZZI + 1093.75 ZZZ \\ & - 1039.07 IZI - 1536.13 IXX - 787.44 IYY \\ & + 1052.87 ZXX + 520.69 ZYY - 350.32 XIX \\ & + 133.81 XZX - 350.32 YIY + 133.81 YZY \\ & - 701.5 XXX + 359.17 XYY - 359.17 YXY \\ & - 701.5 YYX - 1911.94 IIX + 297.03 IZX \\ & + 1090.4 ZIX + 259.3 ZZX + 62.31 XII \\ & - 15.69 XIZ - 31.35 XZI + 3.86 XZZ \\ & + 263.80 IXI - 11.88 IXZ - 199.39 ZXI \\ & - 19.39 ZXZ + 125.97 XXI - 31.25 XXZ \\ & + 125.97 YYI - 31.25 YYZ , \end{aligned}$$

and

$$\begin{aligned} H_{\text{ordered}} & = 8503.93 III - 1093.75 IIZ - 2187.51 IZI \\ & - 4375.01 ZII - 1536.13 IXX - 787.43 IYY \\ & + 1052.87 ZXX + 520.69 ZYY - 350.32 XIX \\ & + 133.81 XZX - 350.32 YIY + 133.81 YZY \\ & - 701.5 XXX + 359.17 XYY - 359.17 YXY \\ & - 701.5 YYX - 2379.65 IIX + 764.74 IZX \\ & + 1558.14 ZIX - 208.4 ZZX + 62.31 XII \\ & - 15.69 XIZ - 31.35 XZI + 3.86 XZZ \\ & + 314.43 IXI - 62.51 IXZ - 250.02 ZXI \\ & + 31.24 ZXZ + 125.97 XXI - 31.25 XXZ \\ & + 125.97 YYI - 31.25 YYZ + 23.44 IZZ \\ & + 46.88 ZIZ + 93.75 ZZI , \end{aligned}$$

which are obviously different, as expected from our previous analysis. In this, we used an energy scaling factor $\hbar\omega \equiv 2000 \text{ cm}^{-1}$ and, for notational simplicity, we dropped out the Kronecker direct product symbol and omitted the qubit indices within the ordered strings.

- [1] Y. Cao, J. Romero, J. P. Olson, M. Degroote, P. D. Johnson, M. Kieferová, I. D. Kivlichan, T. Menke, B. Peropadre, N. P. D. Sawaya, S. Sim, L. Veis, and A. Aspuru-Guzik, Quantum chemistry in the age of quantum computing, *Chem. Rev.* **119**, 10856 (2019).
- [2] P. J. J. O'Malley, R. Babbush, I. D. Kivlichan, J. Romero, J. R. McClean, R. Barends, J. Kelly, P. Roushan, A. Tranter, N. Ding, B. Campbell, Y. Chen, Z. Chen, B. Chiaro, A. Dunsworth, A. G. Fowler, E. Jeffrey, E. Lucero, A. Megrant, J. Y. Mutus, M. Neeley, C. Neill, C. Quintana, D. Sank, A. Vainsencher, J. Wenner, T. C. White, P. V. Coveney, P. J. Love, H. Neven, A. Aspuru-Guzik, and J. M. Martinis, Scalable quantum simulation of molecular energies, *Phys. Rev. X* **6**, 031007 (2016).
- [3] B. P. Lanyon, J. D. Whitfield, G. G. Gillett, M. E. Goggin, M. P. Almeida, I. Kassal, J. D. Biamonte, M. Mohseni, B. J. Powell, M. Barbieri, A. Aspuru-Guzik, and A. G. White, Towards quantum chemistry on a quantum computer, *Nature Chem* **2**, 106 (2010).
- [4] Google AI Quantum and Collaborators, F. Arute, K. Arya, R. Babbush, D. Bacon, J. C. Bardin, R. Barends, S. Boixo, M. Broughton, B. B. Buckley, D. A. Buell, B. Burkett, N. Bushnell, Y. Chen, Z. Chen, B. Chiaro, R. Collins, W. Courtney, S. Demura, A. Dunsworth, E. Farhi, A. Fowler, B. Foxen, C. Gidney, M. Giustina, R. Graff, S. Habegger, M. P. Harrigan, A. Ho, S. Hong, T. Huang, W. J. Huggins, L. Ioffe, S. V. Isakov, E. Jeffrey, Z. Jiang, C. Jones, D. Kafri, K. Kechedzhi, J. Kelly, S. Kim, P. V. Klimov, A. Korotkov, F. Kostritsa, D. Landhuis, P. Laptev, M. Lindmark, E. Lucero, O. Martin, J. M. Martinis, J. R. McClean, M. McEwen, A. Megrant, X. Mi, M. Mohseni, W. Mroczkiewicz, J. Mutus, O. Naaman, M. Neeley, C. Neill, H. Neven, M. Y. Niu, T. E. O'Brien, E. Ostby, A. Petukhov, H. Putterman, C. Quintana, P. Roushan, N. C. Rubin, D. Sank, K. J. Satzinger, V. Smelyanskiy, D. Strain, K. J. Sung, M. Szalay, T. Y. Takeshita, A. Vainsencher, T. White, N. Wiebe, Z. J. Yao, P. Yeh, and A. Zalcman, Hartree-fock on a superconducting qubit quantum computer, *Science* **369**, 1084 (2020), <https://www.science.org/doi/pdf/10.1126/science.abb9811>.
- [5] M. Rossmannek, F. Pavošević, A. Rubio, and I. Tavernelli, Quantum embedding method for the simulation of strongly correlated systems on quantum computers, *J. Phys. Chem. Lett.* **14**, 3491 (2023).
- [6] H. L. Tang, V. Shkolnikov, G. S. Barron, H. R. Grimsley, N. J. Mayhall, E. Barnes, and S. E. Economou, Qubit-adapt-vqe: An adaptive algorithm for constructing hardware-efficient ansätze on a quantum processor, *PRX Quantum* **2**, 020310 (2021).
- [7] J. Romero, R. Babbush, J. R. McClean, C. Hempel, P. J. Love, and A. Aspuru-Guzik, Strategies for quantum computing molecular energies using the unitary coupled cluster ansatz, *Quantum Sci. Technol.* **4**, 014008 (2018).
- [8] N. P. D. Sawaya, F. Paesani, and D. P. Tabor, Near- and long-term quantum algorithmic approaches for vibrational spectroscopy, *Phys. Rev. A* **104**, 062419 (2021).
- [9] S. McArdle, S. Endo, A. Aspuru-Guzik, S. C. Benjamin, and X. Yuan, Quantum computational chemistry, *Rev. Mod. Phys.* **92**, 015003 (2020).
- [10] P. J. Ollitrault, A. Baiardi, M. Reiher, and I. Tavernelli, Hardware efficient quantum algorithms for vibrational structure calculations, *Chem. Sci.* **11**, 6842–6855 (2020).
- [11] P. Jordan and E. Wigner, Über das paulische äquivalenzverbot, *Z. Phys.* **47**, 631 (1928).
- [12] G. C. Wick, The evaluation of the collision matrix, *Phys. Rev.* **80**, 268 (1950).
- [13] A. Macridin, P. Spentzouris, J. Amundson, and R. Harnik, Digital quantum computation of fermion-boson interacting systems, *Phys. Rev. A* **98**, 042312 (2018).
- [14] M. Tudorovskaya and D. Muñoz Ramo, Quantum computing simulation of a mixed spin-boson hamiltonian and its performance for a cavity quantum electrodynamics problem, *Phys. Rev. A* **109**, 032612 (2024).
- [15] R. Somma, G. Ortiz, E. Knill, and J. Gubernatis, Quantum simulations of physics problems, *Int. J. Quantum Inf.* **01**, 189 (2003).
- [16] X.-Y. Huang, L. Yu, X. Lu, Y. Yang, D.-S. Li, C.-W. Wu, W. Wu, and P.-X. Chen, *Qubitization of bosons* (2022), [arXiv:2105.12563 \[quant-ph\]](https://arxiv.org/abs/2105.12563).
- [17] H. A. Buchdahl, Concerning a Kind of Truncated Quantized Linear Harmonic Oscillator, *Am. J. Phys.* **35**, 210 (1967), https://pubs.aip.org/aapt/ajp/article-pdf/35/3/210/10112561/210.1_online.pdf.
- [18] M. Carvajal, R. Lemus, A. Frank, C. Jung, and E. Ziemniak, An extended su(2) model for coupled morse oscillators, *Chem. Phys.* **260**, 105 (2000).
- [19] U. E. Khodaeva, D. L. Kovrizhin, and J. Knolle, Quantum simulation of the one-dimensional fermi-hubbard model as a z_2 lattice-gauge theory, *Phys. Rev. Res.* **6**, 013032 (2024).
- [20] D. M. Dennison and G. E. Uhlenbeck, The two-minima problem and the ammonia molecule, *Phys. Rev.* **41**, 313 (1932).
- [21] J. Ricardo Letelier and C. A. Utreras-Díaz, A numerical molecular potential for the umbrella inversion in ammonia, *Spectrosc. Acta A* **53**, 247 (1997).
- [22] H. V. L. Nguyen, Quantum tunneling: History and mystery of large amplitude motions over a century, *J. Phys. Chem. Lett.* **16**, 104 (2025).
- [23] D. Lauvergnat and A. Nauts, Smolyak scheme for solving the schrödinger equation: Application to malonaldehyde in full dimensionality, *ChemPhysChem* **24**, e202300501 (2023), <https://chemistry-europe.onlinelibrary.wiley.com/doi/pdf/10.1002/cphc.202300501>.
- [24] N. P. D. Sawaya, T. Menke, T. H. Kyaw, S. Johri, A. Aspuru-Guzik, and G. G. Guerreschi, Resource-efficient digital quantum simulation of d-level systems for photonic, vibrational, and spin-s hamiltonians, *npj Quantum Inf.* **6**, 49 (2020).
- [25] N. Chancellor, Domain wall encoding of discrete variables for quantum annealing and qaoa, *Quantum Sci. Technol.* **4**, 045004 (2019).
- [26] M. R. Geller, J. M. Martinis, A. T. Sornborger, P. C. Stancil, E. J. Pritchett, H. You, and A. Galiaudtinov, Universal quantum simulation with prethreshold superconducting qubits: Single-excitation subspace method, *Phys. Rev. A* **91**, 062309 (2015).
- [27] G. Stock and M. Thoss, Semiclassical description of nonadiabatic quantum dynamics, *Phys. Rev. Lett.* **78**, 578

- (1997).
- [28] M. Thoss and G. Stock, Mapping approach to the semiclassical description of nonadiabatic quantum dynamics, *Phys. Rev. A* **59**, 64 (1999).
- [29] H. Meyer and W. H. Miller, Classical models for electronic degrees of freedom: Derivation via spin analogy and application to $f^*+h_2 \rightarrow f+h_2$, *J. Chem. Phys.* **71**, 2156 (1979), https://pubs.aip.org/aip/jcp/article-pdf/71/5/2156/18918973/2156.1_online.pdf.
- [30] C. D. Batista and G. O. and, Algebraic approach to interacting quantum systems, *Adv. Phys.* **53**, 1 (2004).
- [31] B. Toloui and P. J. Love, Quantum algorithms for quantum chemistry based on the sparsity of the ci-matrix (2013), [arXiv:1312.2579](https://arxiv.org/abs/1312.2579) [quant-ph].
- [32] R. Babbush, D. W. Berry, Y. R. Sanders, I. D. Kivlichan, A. Scherer, A. Y. Wei, P. J. Love, and A. Aspuru-Guzik, Exponentially more precise quantum simulation of fermions in the configuration interaction representation, *Quantum Sci. Technol.* **3**, 015006 (2017).
- [33] Y. Shee, P.-K. Tsai, C.-L. Hong, H.-C. Cheng, and H.-S. Goan, Qubit-efficient encoding scheme for quantum simulations of electronic structure, *Phys. Rev. Res.* **4**, 023154 (2022).
- [34] B. Senjean, S. Yalouz, and M. Saubanère, Toward density functional theory on quantum computers?, *SciPost Phys.* **14**, 055 (2023).
- [35] H. Singh, S. Majumder, and S. Mishra, Hückel molecular orbital theory on a quantum computer: A scalable system-agnostic variational implementation with compact encoding, *J. Chem. Phys.* **160**, 194106 (2024).
- [36] M. Stroeks, D. Lenterman, B. Terhal, and Y. Herasymenko, Solving free fermion problems on a quantum computer (2024), [arXiv:2409.04550](https://arxiv.org/abs/2409.04550) [quant-ph].
- [37] I. Burghardt, R. Carles, C. F. Kammerer, B. Lasorne, and C. Lasser, Dynamical approximations for composite quantum systems: assessment of error estimates for a separable ansatz, *J. Phys. A* **55**, 224010 (2022).
- [38] A. Javadi-Abhari, M. Treinish, K. Krsulich, C. J. Wood, J. Lishman, J. Gacon, S. Martiel, P. D. Nation, L. S. Bishop, A. W. Cross, B. R. Johnson, and J. M. Gambetta, Quantum computing with Qiskit (2024), [arXiv:2405.08810](https://arxiv.org/abs/2405.08810) [quant-ph].
- [39] E. Anderson, Z. Bai, C. Bischof, S. Blackford, J. Demmel, J. Dongarra, J. Du Croz, A. Greenbaum, S. Hammarling, A. McKenney, and D. Sorensen, *LAPACK Users' Guide*, 3rd ed. (Society for Industrial and Applied Mathematics, Philadelphia, PA, 1999).
- [40] J.-L. Chang, A new formula to calculate franck-CONDON factors for displaced and distorted harmonic oscillators, *J. Mol. Spectrosc.* **232**, 102 (2005).
- [41] D. Wecker, B. Bauer, B. K. Clark, M. B. Hastings, and M. Troyer, Gate-count estimates for performing quantum chemistry on small quantum computers, *Phys. Rev. A* **90**, 022305 (2014).
- [42] V. von Burg, G. H. Low, T. Häner, D. S. Steiger, M. Reiher, M. Roetteler, and M. Troyer, Quantum computing enhanced computational catalysis, *Phys. Rev. Res.* **3**, 033055 (2021).
- [43] J. Lee, D. W. Berry, C. Gidney, W. J. Huggins, J. R. McClean, N. Wiebe, and R. Babbush, Even more efficient quantum computations of chemistry through tensor hypercontraction, *PRX Quantum* **2**, 030305 (2021).
- [44] E. Koridon, S. Yalouz, B. Senjean, F. Buda, T. E. O'Brien, and L. Visscher, Orbital transformations to reduce the 1-norm of the electronic structure hamiltonian for quantum computing applications, *Phys. Rev. Res.* **3**, 033127 (2021).
- [45] P. Jordan, Der zusammenhang der symmetrischen und linearen gruppen und das mehrkörperproblem, *Z. Physik* **94**, 531 (1935).
- [46] J. Schwinger, On angular momentum, *Unpublished Report*, Number NYO (1952).
- [47] T. Holstein and H. Primakoff, Field dependence of the intrinsic domain magnetization of a ferromagnet, *Phys. Rev.* **58**, 1098 (1940).
- [48] Y. Qiao and F. Grossmann, Exact variational dynamics of the multimode bose-hubbard model based on $SU(m)$ coherent states, *Phys. Rev. A* **103**, 042209 (2021).